Contents lists available at **CEPM**

Computational Engineering and Physical Modeling

Journal homepage: www.jcepm.com

On the Study of Magnetohydrodynamic Squeezing Flow of Nanofluid between Two Parallel Plates Embedded in a Porous Medium

M.G. Sobamowo[1], L.O. Jayesimi[2], M.A. Waheed[3]

1. Department of Mechanical Engineering, University of Lagos, Akoka, Lagos, Nigeria
2. Works and Physical Planning Department, University of Lagos, Akoka, Lagos, Nigeria
3. Department of Mechanical Engineering, Federal University of Agriculture, Abeokuta, Nigeria

Corresponding author: *mikegbeminiyiprof@yahoo.com*

https://doi.org/10.22115/CEPM.2018.122325.1013

ARTICLE INFO

Article history:
Received: 11 March 2018
Revised: 20 June 2018
Accepted: 21 June 2018

Keywords:
Squeezing flow;
Nanofluid;
Magnetic field;
Parallel plates;
Differential transformation method.

ABSTRACT

A study of magnetohydrodynamic squeezing flow of nanofluid between two parallel plates embedded in a porous medium is presented in this work. The ordinary differential equation which is transformed from the developed governing partial differential equations is solved using differential transformation method. The accuracy of the results of the approximate analytical method are established as they agree very well with the results numerical method using fourth-fifth order Runge-Kutta-Fehlberg method. Using the developed analytical solutions, the parametric studies reveal that when the velocity of the flow increases during the squeezing process, the Hartmann and squeezing numbers decrease while during the separation process, the velocity of the fluid increases with increase in Hartmann and squeezing numbers. Also, the velocity of the nanofluids further decreases as the Hartmann number increases when the plates move apart. However, it is revealed that increase in nanotube concentration leads to an increase in the velocity of the flow during the squeezing flow. The present study will be useful in various industrial, biological and engineering applications.

How to cite this article: Sobamowo GM, Jayesimi O, Waheed A. On the study of magnetohydrodynamic squeezing flow of nanofluid between two parallel plates embedded in a porous medium. Comput Eng Phys Model 2018;1(4):1–15. https://doi.org/10.22115/CEPM.2018.122325.1013

1. Introduction

The various industrial, biological and engineering applications of flow of squeezing flow of fluid between parallel plates have been the impetus for the continued interest and generation renewed interests on the subject. Also, the continuous technological developments have shown the various industrial, biological and engineering applications etc. These various applications coupled with the practical significance of the phenomena have in recent times made the process an increasing area of an active research fields in fluid dynamics. Although, the pioneer work and the basic formulations on the flow phenomena was carried out Stefan [1], the analysis of the squeezing flow process has continued to receive tremendous attention in the past few decades. However, the applications of Reynolds equation for the squeezing flow analysis in earlier studies [1–3] led the studies to insufficient and inaccurate analyses as shown by Jackson [4] and Usha and Sridharan [5]. Consequently, further studies have been presented in recent times to give a better insight into the flow phenomena. Among these study, Usha and Sridharan [5] investigated the arbitrary squeezing flow of a viscous fluid between elliptic plates while in an earlier work, Yang [6] considered unsteady laminar boundary layers in an incompressible stagnation flow. In a group of research studies, Kuzma [7], Tichy and Winer [8] and Grimm [9] examined the effects of fluid inertial on squeezing flow. Moreover, in order to gain better insight into the flow process, further works has been done [5–15].

Analyses of unsteady squeezing flow of Casson and viscous fluids between two plates have been carried out by Khan [10] and Rashidi et al. [16], respectively. Effects of heat transfer on the squeezing flow characteristics of viscous fluid was investigated by Duwairi et al. [17] while Qayyum et al. [18] analyzed the squeezing flow pattern of second grade and micropolar fluids. The squeezing flow behaviour of dusty fluids was examined by Hamdam and Baron [14]. The flow heat transfer of viscous fluid on a porous surface of a squeezing flow problem was presented by Mahmood [19]. Using differential transformation method, approximate analytical solutions were developed by Hatami and Jing [20] to study the squeezing flow of Newtonian and non-Newtonian nanofluids. An extended work on heat and mass transfer of a rotating squeezing flow of nanofluid was submitted by Mohyud-Din et al. [21]. In another work [22], the authors scrutinized the squeezing flow of Casson fluid under the impacts of effects of thermal radiation. Qayyum and Khan [23] investigated the squeezing problem immersed in a porous medium while Qayyum et al. [24]studied the influence of slip on the unsteady axisymmetric squeezing flow of viscous fluid through a porous medium channel. A study on heat and mass transfer in the unsteady squeezing flow between parallel plates by Mustafa et al.[25]. In different studies, the effects of magnetic field on the steady and unsteady squeezing flow of different Newtonian and Non-Newtonian fluids have been examined by Siddiqui et al.[26], Domairry and Aziz [27], Acharya et al. [28], Ahmed et al. [29], Ahmed et al. [30], Khan et al. [31,32], Hayat et al. [33], Khan et al. [34], Ullah et al. [35] etc. In a recent study, combined effects of slip and magnetic field on the squeezing flow problem was studied by Sobamowo and Jayesimi [36] using Chebychev spectral collocation method. In a previous study, methods such as regular and singular perturbation and differential transformation has been used by Sobamowo and Akinshilo [37] and Sobamowo [38] to analyze such flow problem under the magnetic field. Effects of nanoparticle shapes and Ferro-magnetic magnetic field on peristaltic flow of Copper-water by

Akbar and Butt [39] while Sheikholesmi and Bhatti [40] examined the impacts of magnetic field and shape of nanoparticles on the heat transfer characteristic of nanofluid. Further studies on the effects of magnetic fields, thermal radiation, nanoparticles, chemical reactions etc. are presented in [41–49].

In the past and recent studies, different numerical and analytical approximate methods have been adopted to analyze the nonlinear problems of the flow processes. In the present study, differential transformation method is used to analyze the magnetohydrodynamic squeezing flow of nanofluid between two parallel plates embedded in a porous medium. Parametric studies are carried out using the approximate analytical solutions.

2. Description of the problem and model development

Fig. 1 shows an unsteady two-dimensional squeezing flow of nanofluid between two parallel plates placed at time-variant distance and under the influence of magnetic field. In such flow problem as presented in the figure, it is assumed that the flow of the nanofluid is laminar, stable, incompressible, isothermal, non-reacting chemically, the nanoparticles and base fluid are in thermal equilibrium and the physical properties are constant. The fluid conducts electrical energy as it flows unsteadily under magnetic force field. The fluid structure is everywhere in thermodynamic equilibrium and the plate is maintained at constant temperature.

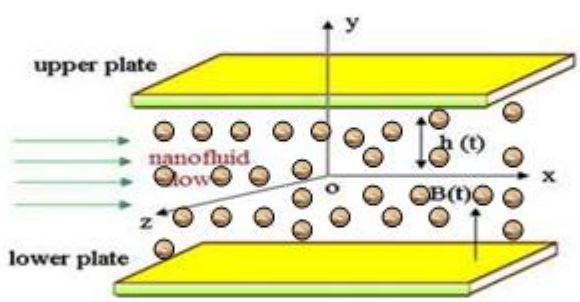

Fig. 1. Model diagram of the flow process.

Following the assumptions, the governing equations for the flow are given as [36–38]

$$\frac{\partial \bar{u}}{\partial x}+\frac{\partial \bar{u}}{\partial y} \tag{1}$$

$$\rho_{nf}\left(\frac{\partial \bar{u}}{\partial t}+\bar{u}\frac{\partial \bar{u}}{\partial x}+v\frac{\partial \bar{u}}{\partial y}\right)=-\frac{\partial p}{\partial x}+\mu_{nf}\left(\frac{\partial^2 \bar{u}}{\partial x^2}+\frac{\partial^2 \bar{u}}{\partial y^2}\right)-\sigma B_o^2\bar{u}-\frac{\mu_{nf}\bar{u}}{K_p} \tag{2}$$

$$\rho_{nf}\left(\frac{\partial \bar{v}}{\partial t}+\bar{u}\frac{\partial \bar{v}}{\partial x}+\bar{v}\frac{\partial \bar{v}}{\partial y}\right)=-\frac{\partial p}{\partial y}+\mu_{nf}\left(\frac{\partial^2 \bar{v}}{\partial x^2}+\frac{\partial^2 \bar{v}}{\partial y^2}\right)-\frac{\mu_{nf}\bar{v}}{K_p} \tag{3}$$

where

$$\rho_{nf}=\rho_f\left(1-\phi\right)+\rho_s\phi \tag{4-a}$$

$$\mu_{nf} = \frac{\mu_f}{(1-\phi)^{2.5}} \quad \text{(Brinkman model)} \tag{4-b}$$

and the magnetic field parameter is given as

$$B(t) = \frac{B_0}{\sqrt{1-\alpha t}} \tag{5}$$

Under the assumption of no-slip condition, the prevailing boundary conditions are stated as

$$y = h(t) = H\sqrt{1-at}, \quad \bar{u} = 0, \quad \bar{v} = -V_w, \quad \begin{array}{l} y = 0, \quad \dfrac{\partial \bar{u}}{\partial y} = 0, \quad v = 0 \\ x = 0, \quad u = 0 \end{array} \tag{6}$$

Table 1 and 2 present the thermal-physical properties of the base fluid and the nanoparticles, respectively

Table 1
Thermal-physical properties of the base fluid [39–41][50,51].

Base fluid	ρ (kg/m^3)	c_p (J/kgK)	k (W/mK)
Pure water	997.1	4179	0.613
Engine oil	884	1910	0.144
Kerosene	783	2010	0.145
Ethylene Glycol	1115	2430	0253

Table 2
Thermal-physical properties of nanoparticles [39–41][50,51].

Nanoparticles	ρ (kg/m^3)	c_p (J/kgK)	k (W/mK)
Copper (Cu)	8933	385	401
Silver (Ag)	10500	235.0	429
SWCNTs	2600	42.5	6600
Aluminum oxide (Al_2O_3)	3970	765	40
Copper (II) Oxide (CuO)	783	540	18
Titanium dioxide (TiO_2)	4250	686.2	8.9538

Introducing the following dimensionless and similarity variables into Eq. (1) - (3).

$$\begin{gathered} \bar{u} = \frac{\alpha x}{(1-\alpha t)^{0.5}} f'(\eta,t), \quad \bar{v} = -\frac{\alpha x}{(1-\alpha t)^{0.5}} f(\eta,t), \quad \eta = \frac{y}{H(1-\alpha t)^{0.5}} \\ Re = -SA(1-\phi)^{2.5} = \frac{\rho_{nf} H V_w}{\mu_{nf}}, \quad S = \frac{\alpha H^2}{2v_f}, \quad Da = \frac{K_p}{H^2}, \quad A = (1-\phi) + \phi\frac{\rho_s}{\rho_f} \end{gathered}, \tag{7}$$

one arrives at

$$f^{iv} + Re(\eta f''' + 3f'' + ff''' - ff'') - M^2 f'' - \frac{1}{Da} f'' = 0 \tag{8}$$

Alternatively, Eq. (8) can also be expressed as

$$f^{iv} - SA(1-\phi)^{2.5}\left(\eta f''' + 3f'' + ff''' - f'f''\right) - M^2 f'' - \frac{1}{Da} f'' = 0 \tag{9}$$

and the boundary conditions are

$$f(0) = 0, \quad f''(0) = 0$$

$$f(1) = 1, \quad f'(1) = 0 \tag{10}$$

The boundary conditions depict the condition of no-slip on the disk.

3. Analysis of the differential equation using differential transform method

The developed nonlinear equation in Eq. (9) cannot be solved exactly and analytically. However, we apply an approximated analytical method such as differential transformation method (DTM) as introduced by Zhou [52] to solve the equation. The basic definitions, the properties and some applications of the method can be found in [38,53–57]

Using the DTM operational properties as stated in [38,52–57], the differential transform of Eq. (8) is

$$\begin{aligned}&(m+1)(m+2)(m+3)(m+4)F(m+4)\\ &+Re\begin{bmatrix} +3(m+1)(m+2)F(m+2)+ \\ \sum_{l=0}^{m}\delta(l)(m-l+1)(m-l+2)(m-l+3)F(m-l+3) \\ +\sum_{l=0}^{m}F(m-l)(l+1)(l+2)(l+3)F(l+3) \\ -\sum_{l=0}^{m}(m-l+1)F(m-l+1)(l+1)(l+2)F(l+2) \end{bmatrix} - \left(M^2+\frac{1}{Da}\right)(m+1)(m+2)F(m+2) = 0\end{aligned} \tag{15}$$

where

$$\delta(l) = \begin{cases} 1 & l = 1 \\ 0 & l \neq 0 \end{cases}$$

The boundary conditions are

$$F(0) = 0, \quad (m+1)(m+2)F(m+2) = 0 \quad \Rightarrow m = 0, \quad F(2) = 0$$

$$\sum_{l=0}^{m} F(m) = 1, \quad \Rightarrow m = 1, \quad F(1) = k_1,$$

$$\sum_{l=0}^{m} (m+1)F(m+1) = 0, \quad \Rightarrow m = 2, \quad F(3) = k_2 \tag{16}$$

Therefore, we have the following boundary conditions in DTM domain

$$F(0)=0, \quad F(2)=0, \quad F(1)=k_1, \quad F(3)=k_2 \tag{17}$$

where k_1 and k_2 are the constants which will be determined through the boundary conditions

$$F(m+4)=\frac{1}{(m+1)(m+2)(m+3)(m+4))}\left\{\begin{array}{l}\left(M^2+\frac{1}{Da}\right)(m+1)(m+2)F(m+2)\\ -Re\sum_{l=0}^{m}\delta(l)(m-l+1)(m-l+2)(m-l+3)F(m-l+3)\\ -3Re(m+1)(m+2)F(m+2)\\ -Re\sum_{l=0}^{m}F(m-l)(l+1)(l+2)(l+3)F(l+3)\\ -Re\sum_{l=0}^{m}(m-l+1)F(m-l+1)(l+1)(l+2)F(l+2)\end{array}\right\} \tag{18}$$

Using *m=0, 1, 2, 3…* in the above recursive relations, one arrives at

$$F(4)=0$$

$$F(5)=\frac{1}{20}\left(\left(M^2+\frac{1}{Da}\right)k_2-3Rek_1\right)$$

$$F(6)=0$$

$$F(7)=\frac{1}{840}\left\{\left(M^2+\frac{1}{Da}\right)\left(\left(M^2+\frac{1}{Da}\right)k_2-3Rek_1\right)+\left(9Re^2k_2+12Rek_2^2+6Re^3k_1k_2\right)\right\}$$

$$F(8)=0$$

$$F(9)=\frac{1}{60480}\left\{\begin{array}{l}\left(M^2+\frac{1}{Da}\right)\left\{\begin{array}{l}\left(M^2+\frac{1}{Da}\right)\left(\left(M^2+\frac{1}{Da}\right)k_2-3Rek_1\right)\\ +\left(9Re^2k_2+12Rek_2^2+6Re^3k_1k_2\right)\end{array}\right\}\\ -\left(\begin{array}{l}27Re^3k_2+108Re^2k_2^2+54Re^3k_1k_2+48k_1k_2Re^2\\ +48Rek_1k_2^2+24Re^2k_1k_0^2\end{array}\right)\end{array}\right\} \tag{19}$$

$$F(10)=0$$

Following from above and according to the definition of DTM, one can write the solution of Eq. (8) as

$$\begin{aligned}f(\eta)=&k_1\eta+k_2\eta^3+\frac{1}{20}\left(\left(M^2+\frac{1}{Da}\right)k_2-3Rek_1\right)\eta^5+\frac{1}{840}\left\{\begin{array}{l}\left(M^2+\frac{1}{Da}\right)\left(\left(M^2+\frac{1}{Da}\right)k_2-3Rek_1\right)\\ +\left(9Re^2k_2+12Rek_2^2+6Re^2k_1k_2\right)\end{array}\right\}\eta^7\\ &+\frac{1}{60480}\left\{\begin{array}{l}\left(M^2+\frac{1}{Da}\right)\left\{\left(M^2+\frac{1}{Da}\right)\left(\left(M^2+\frac{1}{Da}\right)k_2-3Rek_1\right)+\left(9\alpha^2k_2+12Rek_2^2+6k_1k_2Re^3\right)\right\}\\ -\left(27Re^3k_2+108Re^2k_2^2+54Re^3k_1k_2+48k_1k_2Re^2+48Rek_1k_2^2+24Re^2k_1k_0^2\right)\end{array}\right\}\eta^9\\ &+\ldots\end{aligned} \tag{20}$$

The unknown values of constants k_1 and k_2 can be found using Eq. (15) which states that at $f(1)=1, \quad f'(1)=0$. Therefore, according to the boundary conditions, we have

$$f(1)=k_1+k_2+\frac{1}{20}\left(\left(M^2+\frac{1}{Da}\right)k_2-3Rek_1\right)+\frac{1}{840}\left\{\begin{array}{l}\left(M^2+\frac{1}{Da}\right)\left(\left(M^2+\frac{1}{Da}\right)k_2-3Rek_1\right)\\ +\left(9Re^2k_2+12Rek_2^2+6Re^2k_1k_2\right)\end{array}\right\}$$
$$+\frac{1}{60480}\left\{\begin{array}{l}\left(M^2+\frac{1}{Da}\right)\left\{\left(M^2+\frac{1}{Da}\right)\left(\left(M^2+\frac{1}{Da}\right)k_2-3Rek_1\right)+\left(9\alpha^2k_2+12Rek_2^2+6k_1k_2Re^3\right)\right\}\\ -\left(27Re^3k_2+108Re^2k_2^2+54Re^3k_1k_2+48k_1k_2Re^2+48Rek_1k_2^2+24Re^2k_1k_0^2\right)\end{array}\right\}$$
$$+\ldots=1 \tag{21}$$

$$f'(1)=k_1+3k_2+\frac{1}{4}\left(\left(M^2+\frac{1}{Da}\right)k_2-3Rek_1\right)+\frac{1}{120}\left\{\begin{array}{l}\left(M^2+\frac{1}{Da}\right)\left(\left(M^2+\frac{1}{Da}\right)k_2-3Rek_1\right)\\ +\left(9Re^2k_2+12Rek_2^2+6Re^2k_1k_2\right)\end{array}\right\}$$
$$+\frac{1}{6720}\left\{\begin{array}{l}\left(M^2+\frac{1}{Da}\right)\left\{\left(M^2+\frac{1}{Da}\right)\left(\left(M^2+\frac{1}{Da}\right)k_2-3Rek_1\right)+\left(9\alpha^2k_2+12Rek_2^2+6k_1k_2Re^3\right)\right\}\\ -\left(27Re^3k_2+108Re^2k_2^2+54Re^3k_1k_2+48k_1k_2Re^2+48Rek_1k_2^2+24Re^2k_1k_0^2\right)\end{array}\right\}$$
$$+\ldots=0 \tag{22}$$

It should be noted that when Eq. (21) and (22) are solved, different values for k_1 and k_2 are gotten for respective values of α and Re.

In order to find the skin friction, the second-order derivatives of $f(1)$ at the wall is developed as

$$f''(\eta)=6k_2\eta^3+\left(\left(M^2+\frac{1}{Da}\right)k_2-3Rek_1\right)+\frac{1}{20}\left\{\begin{array}{l}\left(M^2+\frac{1}{Da}\right)\left(\left(M^2+\frac{1}{Da}\right)k_2-3Rek_1\right)\\ +\left(9Re^2k_2+12Rek_2^2+6Re^2k_1k_2\right)\end{array}\right\}$$
$$+\frac{1}{840}\left\{\begin{array}{l}\left(M^2+\frac{1}{Da}\right)\left\{\left(M^2+\frac{1}{Da}\right)\left(\left(M^2+\frac{1}{Da}\right)k_2-3Rek_1\right)+\left(9\alpha^2k_2+12Rek_2^2+6k_1k_2Re^3\right)\right\}\\ -\left(27Re^3k_2+108Re^2k_2^2+54Re^3k_1k_2+48k_1k_2Re^2+48Rek_1k_2^2+24Re^2k_1k_0^2\right)\end{array}\right\}$$
$$+\ldots \tag{23}$$

It should be noted that $Re=-SA(1-\phi)^{2.5}$

Judging from physical point of view, the skin friction is an important physical quantity of interest in the flow analysis of fluid.

The skin friction can be expressed as

$$C_f = \frac{\mu_{nf}\left(\frac{\partial u}{\partial y}\right)_{y=h(t)}}{\rho_{nf} V_w^2} \tag{24}$$

Using the dimensionless variables in Eq. (7), we developed a non-dimensional form of Eq. (24) as

$$C_f^* = \frac{H^2}{x^2(1-\alpha t) Re_x C_f} = A(1-\phi)^{2.5} f''(1) \tag{25}$$

which gives,

$$C_f^* = A(1-\phi)^{2.5}\left\{\begin{array}{l} 6k_2 + \left(\left(M^2+\frac{1}{Da}\right)k_2 - 3Rek_1\right) + \frac{1}{20}\left\{\begin{array}{l}\left(M^2+\frac{1}{Da}\right)\left(\left(M^2+\frac{1}{Da}\right)k_2 - 3Rek_1\right)\\ +\left(9Re^2k_2 + 12Rek_2^2 + 6Re^2k_1k_2\right)\end{array}\right\} \\ +\frac{1}{840}\left\{\begin{array}{l}\left(M^2+\frac{1}{Da}\right)\left\{\left(M^2+\frac{1}{Da}\right)\left(\left(M^2+\frac{1}{Da}\right)k_2 - 3Rek_1\right) + \left(9\alpha^2k_2 + 12Rek_2^2 + 6k_1k_2Re^3\right)\right\}\\ -\left(27Re^3k_2 + 108Re^2k_2^2 + 54Re^3k_1k_2 + 48k_1k_2Re^2 + 48Rek_1k_2^2 + 24Re^2k_1k_0^2\right)\end{array}\right\} + \ldots\end{array}\right\} \tag{26}$$

4. Results and discussion

In order to establish the accuracy of the results of the applied approximate analytical method, the results are compared with the results of numerical method (NM) using fourth-fifth order Runge-Kutta-Fehlberg method as presented in Tables 3-5. The table shows the comparisons of results of DTM and NM for different values of permeation Reynolds and Hartmann numbers. Also, the Tables presented the various impacts of controlling flow parameters on the squeezing flow process. It is shown that during the separation flow, the velocity of the flow increases while the skin friction coefficient decreases. However, in the squeezing flow process, increase in the squeezing and Hartmann numbers cause the skin friction coefficient to decrease.

Table 3
Results of NM and DTM for large squeezing number in the absence of magnetic field.

f	*Squeezing S= 101*	*M=0, 1/Da=0*
η	NM	DTM
0.0	0.00000	0.00000
0.1	0.16377	0.16376
0.2	0.32193	0.32194
0.3	0.46995	0.46992
0.4	0.60424	0.60422
0.5	0.72190	0.72191
0.6	0.82063	0.82063
0.7	0.89871	0.89874
0.8	0.95498	0.95496
0.9	0.98878	0.98875
1.0	1.00000	1.00000

Table 4
Results of NM and DTM of skin friction parameter for large separation number under the influence of magnetic field.

$f''(1)$			
S	M	NM	DTM
12.957	6.445	-4.78	-4.78
18.638	6.103	-4.07	-4.07
25.747	7.151	-4.11	-4.11
41.818	11.419	-5.10	-5.10
50.460	9.964	-4.16	-4.16
62.485	11.077	-4.17	-4.17
76.326	12.233	-4.18	4.18

Table 5
Results of NM and DTM for small squeezing number in the absence of magnetic field.

f	*Squeezing S = 0.5, M=0, 1/Da=0*		*Squeezing S = 1.5, M=0, 1/Da=0*	
η	NM	DTM	NM	DTM
0.0	0.00000	0.00000	0.00000	0.00000
0.2	0.31707	0.31705	0.31609	0.31607
0.4	0.59972	0.59971	0.59818	0.59820
0.6	0.81886	0.81884	0.8174	0.81743
0.8	0.95526	0.95525	0.95430	0.95432
1.0	1.00000	1.00000	1.00000	1.00000

Using nanoparticle parameter value of 0.15 i.e. $\phi = 0.15$, Figs. 2 and 3 show the variation of velocities of flow of the fluid over the length. As depicted in the figure, when the axial velocity of fluid flow near the wall region decreases, there is an increase in velocity gradient at the wall region. This behaviour occurs because of the conservativeness of the mass flow rate.

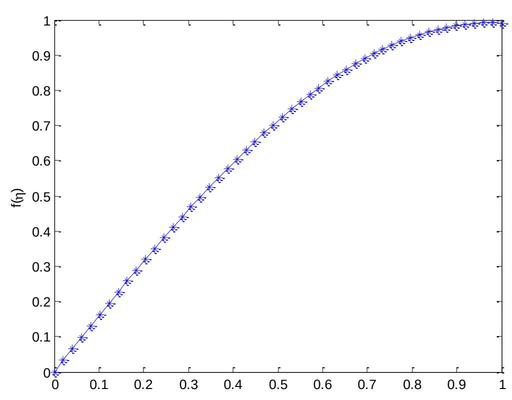

Fig. 2a. Variation of f(η) with the flow length

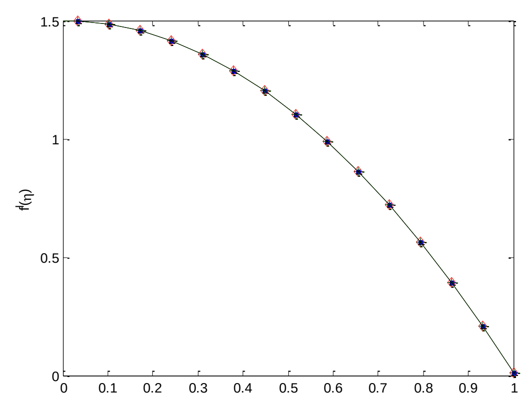

Fig. 2b. Variation of f'(η) with the flow length

Impact of magnetic field parameter on the flow behaviour of the fluid is shown in Fig. 3. As the Hartmann number increases, the flow velocity decreases in the range of $0 \leq \eta \leq 0.5$ and then increases in the range $0.5 < \eta \leq 1$. This is due to the fact that the magnetic field created a retarding force, Lorentz force created which decreases the motion of the fluid at boundary layer during the squeezing flow process. During the separation of the plates, as the magnetic field parameter increases, the flow velocity of the fluid further decreases. Such a behaviour is caused by the fact that the fluid flow with high velocity to fill a vacant space that occurs such that the law of conservation of mass is not violated.

Fig. 4 displays the influence of Darcy number on the squeezing flow pattern of the nanofluid. As it is shown in the figure, there is an opposite trend to that of the squeezing number effects on the flow process. The figure shows that increase in the Darcy number causes the flow velocity to increase in the range of $0 \leq \eta \leq 0.5$ and a decrease is witness in the range $0.5 < \eta \leq 1$.

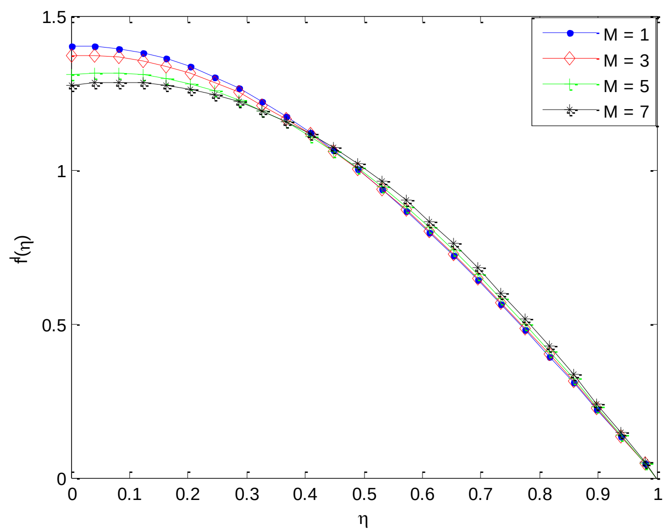

Fig. 3. Effects of magnetic number on the flow velocity of the fluid.

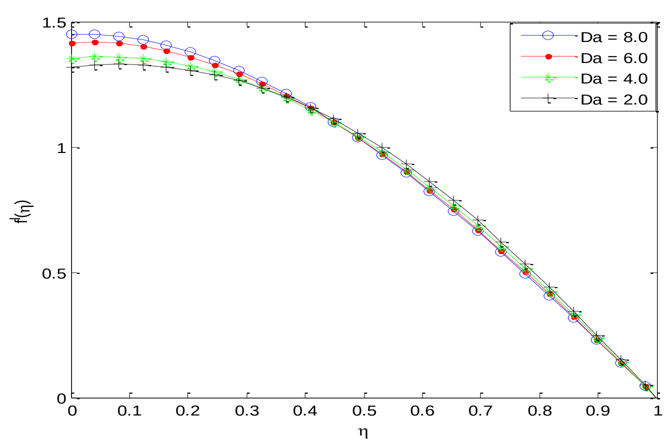

Fig. 4. Effects of Darcy number on the flow velocity of the fluid.

As it is illustrated in Fig. 5, the effects of squeezing number on the flow velocity is shown. As the squeezing number increases, there is a decrease in flow velocity in the range of $0 \leq \eta \leq 0.5$ and then increase in the flow velocity in the range $0.5 < \eta \leq 1$. Fig. 6 shows that impacts of nanoparticle fraction on the fluid velocity. It is shown that as the nanoparticle fraction increases, the velocity decreases in the range of $0 \leq \eta \leq 0.5$ and then increases in the range $0.5 < \eta \leq 1$. This is because increase in the nanoparticle fraction leads to an increased more collisions between nanoparticle and particles at the boundary surface of the plates. Consequently, a retardation in the flow process occurs which decreases the flow velocity near the boundary layer.

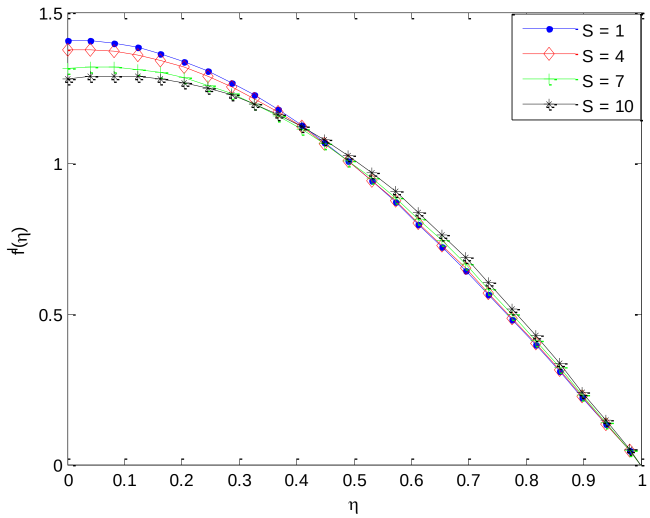

Fig. 5. Effects of Squeezing number on the flow velocity of the fluid.

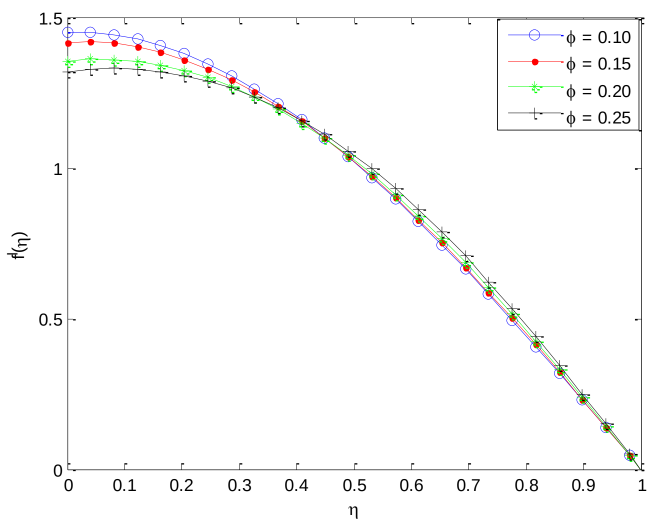

Fig. 6. Effects of nanoparticle fraction on the flow velocity of the fluid.

Table 6
Skin friction for different squeezing, Hartmann and Darcy numbers.

S	M	Da	C_f^*
12.957	4.340	0.475	-3.48
18.638	3.672	0.411	-2.96
25.747	3.587	0.390	-2.99
41.818	7.104	0.232	-3.71
50.460	6.236	0.268	-3.03
62.485	5.820	0.190	-3.03
76.326	6.444	0.173	-3.04

Numerical values for skin friction coefficient are presented in Table 6. The Table also presented the effects of squeezing (S), magnetic parameters (M) and Darcy (Da) on the skin coefficient. It is shown that the numerical value of the skin friction coefficient increases as the squeezing (S) and Hartmann (magnetic field, M) numbers increase, the skin-friction coefficient also increases while the skin-friction coefficient decreases as the Darcy number increases.

5. Conclusion

In this work, analysis of magnetohydrodynamic squeezing flow of nanofluid between two parallel plates embedded in a porous medium have been presented using differential transformation method. The accuracy of the results of the approximate analytical method was established numerically using fourth-fifth order Runge-Kutta-Fehlberg method. Parametric studies were carried out which established the impacts of the controlling flow parameter on the flow process. The present study will be useful in various industrial, biological and engineering applications.

Nomenclature

B(t)	Magnetic field strength
Da	Darcy number
H	Squeezing flow height
Kp	Permeability
M	Hartmann parameter
P	Pressure
py	yield stress of the fluid.
Re	Reynold number
S	Squeezing flow Parameter
U	velocity in x direction
V	velocity in y Direction
v	Dimensionless velocity in y direction
Vw	injection/suction velocity
x	horizontal axis of flow
y	Perpendicular axis to the flow
k_{nf}	Effective thermal conductivity

Greek Symbol

μ_{nf}	Effective dynamic viscosity
ρ_{nf}	Effective density
η	Dimensionless similarity variable
τ	shear stress
τo	Casson yield stress
μ	dynamic viscosity
$\dot{\sigma}$	shear rate
Φ	fraction of nanoparticle in nanofluid

References

[1] Stefan J. Versuche über die scheinbare Adhäsion. Ann Der Phys Und Chemie 1875;230:316–8. doi:10.1002/andp.18752300213.

[2] IV. On the theory of lubrication and its application to Mr. Beauchamp tower's experiments, including an experimental determination of the viscosity of olive oil. Philos Trans R Soc London 1886;177:157–234. doi:10.1098/rstl.1886.0005.

[3] Archibald FR. Load capacity and time relations in squeeze films. Trans ASME J Lub Tech 1956;78:29–35.

[4] Jackson JD. A study of squeezing flow. Appl Sci Res 1963;11:148–52. doi:10.1007/BF03184719.

[5] Usha R, Sridharan R. Arbitrary squeezing of a viscous fluid between elliptic plates. Fluid Dyn Res 1996;18:35–51. doi:10.1016/0169-5983(96)00002-0.

[6] Yang K-T. Un steady laminar boundary layer in an incompressible stagnation flow. ASME J Appl Mech 1958;80:421–7.

[7] Kuzma DC. Fluid inertia effects in squeeze films. Appl Sci Res 1968;18:15–20. doi:10.1007/BF00382330.

[8] Tichy JA, Winer WO. Inertial considerations in parallel circular squeeze film bearings. J Lubr Technol 1970;92:588–92.

[9] Grimm RJ. Squeezing flows of Newtonian liquid films an analysis including fluid inertia. Appl Sci Res 1976;32:149–66. doi:10.1007/BF00383711.

[10] Khan U, Ahmed N, Khan SIU, Bano S, Mohyud-Din ST. Unsteady squeezing flow of a Casson fluid between parallel plates. World J Model Simul 2014;10:308–19.

[11] Birkhoff G, Hydrodynamics A. study in Logic, Fact and Similitude 1960.

[12] Wang CY. The squeezing of a fluid between two plates. J Appl Mech 1976;43:579–83.

[13] Wang CY, Watson LT. Squeezing of a viscous fluid between elliptic plates. Appl Sci Res 1979;35:195–207. doi:10.1007/BF00382705.

[14] Hamdan MH, Barron RM. Analysis of the squeezing flow of dusty fluids. Appl Sci Res 1992;49:345–54. doi:10.1007/BF00419980.

[15] Phan-Thien N. Squeezing flow of a viscoelastic solid. J Nonnewton Fluid Mech 2000;95:343–62. doi:10.1016/S0377-0257(00)00175-0.

[16] Rashidi MM, Shahmohamadi H, Dinarvand S. Analytic Approximate Solutions for Unsteady Two-Dimensional and Axisymmetric Squeezing Flows between Parallel Plates. Math Probl Eng 2008;2008:1–13. doi:10.1155/2008/935095.

[17] Duwairi HM, Tashtoush B, Damseh R. On heat transfer effects of a viscous fluid squeezed and extruded between two parallel plates. Heat Mass Transf 2004. doi:10.1007/s00231-004-0525-5.

[18] Qayyum A, Awais M, Alsaedi A, Hayat T. Unsteady squeezing flow of Jeffery fluid between two parallel disks. Chinese Phys Lett 2012;29:34701.

[19] Mahmood M, Asghar S, Hossain MA. Squeezed flow and heat transfer over a porous surface for viscous fluid. Heat Mass Transf 2007;44:165–73. doi:10.1007/s00231-006-0218-3.

[20] Hatami M, Jing D. Differential Transformation Method for Newtonian and non-Newtonian nanofluids flow analysis: Compared to numerical solution. Alexandria Eng J 2016;55:731–9. doi:10.1016/j.aej.2016.01.003.

[21] Mohyud-Din ST, Zaidi ZA, Khan U, Ahmed N. On heat and mass transfer analysis for the flow of a nanofluid between rotating parallel plates. Aerosp Sci Technol 2015;46:514–22. doi:10.1016/j.ast.2015.07.020.

[22] Mohyud-Din ST, Khan SI. Nonlinear radiation effects on squeezing flow of a Casson fluid between parallel disks. Aerosp Sci Technol 2016;48:186–92. doi:10.1016/j.ast.2015.10.019.

[23] Qayyum M, Khan H. Behavioral study of unsteady squeezing flow through porous medium. J Porous Media 2016;19.

[24] Qayyum M, Khan H, Rahim MT, Ullah I. Modeling and Analysis of Unsteady Axisymmetric Squeezing Fluid Flow through Porous Medium Channel with Slip Boundary. PLoS One 2015;10:e0117368. doi:10.1371/journal.pone.0117368.

[25] Mustafa M, Hayat T, Obaidat S. On heat and mass transfer in the unsteady squeezing flow between parallel plates. Meccanica 2012;47:1581–9. doi:10.1007/s11012-012-9536-3.

[26] Siddiqui AM, Irum S, Ansari AR. UNSTEADY SQUEEZING FLOW OF A VISCOUS MHD FLUID BETWEEN PARALLEL PLATES, A SOLUTION USING THE HOMOTOPY PERTURBATION METHOD. Math Model Anal 2008;13:565–76. doi:10.3846/1392-6292.2008.13.565-576.

[27] Domairry G, Aziz A. Approximate Analysis of MHD Squeeze Flow between Two Parallel Disks with Suction or Injection by Homotopy Perturbation Method. Math Probl Eng 2009;2009:1–19. doi:10.1155/2009/603916.

[28] Acharya N, Das K, Kundu PK. The squeezing flow of Cu-water and Cu-kerosene nanofluids between two parallel plates. Alexandria Eng J 2016;55:1177–86. doi:10.1016/j.aej.2016.03.039.

[29] Ahmed N, Khan U, Khan SI, Xiao-Jun Y, Zaidi ZA, Mohyud-Din ST. Magneto hydrodynamic (MHD) squeezing flow of a Casson fluid between parallel disks. Int J Phys Sci 2013;8:1788–99.

[30] Ahmed N, Khan U, Zaidi ZA, Jan SU, Waheed A, Mohyud-Din ST. MHD flow of an incompressible fluid through porous medium between dilating and squeezing permeable walls. J Porous Media 2014;17.

[31] Khan U, Ahmed N, Khan SI, Zaidi ZA, Xiao-Jun Y, Mohyud-Din ST. On unsteady two-dimensional and axisymmetric squeezing flow between parallel plates. Alexandria Eng J 2014;53:463–8. doi:10.1016/j.aej.2014.02.002.

[32] Khan U, Ahmed N, Zaidi ZA, Asadullah M, Mohyud-Din ST. MHD squeezing flow between two infinite plates. Ain Shams Eng J 2014;5:187–92. doi:10.1016/j.asej.2013.09.007.

[33] Hayat T, Yousaf A, Mustafa M, Obaidat S. MHD squeezing flow of second-grade fluid between two parallel disks. Int J Numer Methods Fluids 2012;69:399–410. doi:10.1002/fld.2565.

[34] Khan H, Qayyum M, Khan O, Ali M. Unsteady Squeezing Flow of Casson Fluid with Magnetohydrodynamic Effect and Passing through Porous Medium. Math Probl Eng 2016;2016:1–14. doi:10.1155/2016/4293721.

[35] Ullah I, Rahim MT, Khan H, Qayyum M. Analytical analysis of squeezing flow in porous medium with MHD effect. Univ Bucharest Sci Bull Ser A Appl Math Phys 2016;78:1223–7027.

[36] Sobamowo GM, Jayesimi LO. Squeezing Flow Analysis of Nanofluid Under the Effects of Magnetic Field and Slip Boundary Conditions Using Chebychev Spectral Collocation Method. Fluid Mech 2017;3:54.

[37] Sobamowo MG, Akinshilo AT. On the analysis of squeezing flow of nanofluid between two parallel plates under the influence of magnetic field. Alexandria Eng J 2018;57:1413–23. doi:10.1016/j.aej.2017.07.001.

[38] Sobamowo MG. Singular perturbation and differential transform methods to two-dimensional flow of nanofluid in a porous channel with expanding/contracting walls subjected to a uniform transverse magnetic field. Therm Sci Eng Prog 2017;4:71–84. doi:10.1016/j.tsep.2017.09.001.

[39] Akbar NS, Butt AW. Ferromagnetic effects for peristaltic flow of Cu–water nanofluid for different shapes of nanosize particles. Appl Nanosci 2016;6:379–85. doi:10.1007/s13204-015-0430-x.

[40] Sheikholeslami M, Bhatti MM. Forced convection of nanofluid in presence of constant magnetic field considering shape effects of nanoparticles. Int J Heat Mass Transf 2017;111:1039–49. doi:10.1016/j.ijheatmasstransfer.2017.04.070.

[41] Ul Haq R, Nadeem S, Khan ZH, Noor NFM. Convective heat transfer in MHD slip flow over a

stretching surface in the presence of carbon nanotubes. Phys B Condens Matter 2015;457:40–7. doi:10.1016/j.physb.2014.09.031.

[42] Rashidi MM, Babu MJ, Sandeep N, Ali ME. MHD Squeezing Flow of Nanofluid Between Parallel Plates in the Presence of Aligned Magnetic Field. J Comput Theor Nanosci 2016;13:8700–8. doi:10.1166/jctn.2016.6033.

[43] Janke VRR, Sugunamma V, Sandeep N. Effect of Nonlinear Thermal Radiation on MHD Flow between Rotating Plates with Homogeneous-Heterogeneous Reactions. Int J Eng Res Africa 2015;20:130–43. doi:10.4028/www.scientific.net/JERA.20.130.

[44] Reddy JVR, Sugunamma V, Sandeep N, Sulochana C. Influence of chemical reaction, radiation and rotation on MHD nanofluid flow past a permeable flat plate in porous medium. J Niger Math Soc 2016;35:48–65. doi:10.1016/j.jnnms.2015.08.004.

[45] Reddy JVR, Sugunamma V, Sandeep N. Simultaneous Effects of Radiation and Variable Heat Source/Sink on MHD Flow of Keosene Fe 3 O 4 Ferroliquid Over a Bidirectional Stretched Geometry. J Nanofluids 2018;7:748–54. doi:10.1166/jon.2018.1490.

[46] Sheikholeslami M, Gorji Bandpy M, Ellahi R, Hassan M, Soleimani S. Effects of MHD on Cu–water nanofluid flow and heat transfer by means of CVFEM. J Magn Magn Mater 2014;349:188–200. doi:10.1016/j.jmmm.2013.08.040.

[47] Sheikholeslami M, Gorji-Bandpy M, Ganji DD, Soleimani S. Heat flux boundary condition for nanofluid filled enclosure in presence of magnetic field. J Mol Liq 2014;193:174–84. doi:10.1016/j.molliq.2013.12.023.

[48] Sheikholeslami M, Gorji-Bandpy M, Ganji DD, Soleimani S, Seyyedi SM. Natural convection of nanofluids in an enclosure between a circular and a sinusoidal cylinder in the presence of magnetic field. Int Commun Heat Mass Transf 2012;39:1435–43. doi:10.1016/j.icheatmasstransfer.2012.07.026.

[49] Sheikholeslami M, Gorji-Bandpy M, Ganji DD, Rana P, Soleimani S. Magnetohydrodynamic free convection of Al2O3–water nanofluid considering Thermophoresis and Brownian motion effects. Comput Fluids 2014;94:147–60. doi:10.1016/j.compfluid.2014.01.036.

[50] Talley LD. Descriptive physical oceanography: an introduction. Academic press; 2011.

[51] Pastoriza-Gallego M, Lugo L, Legido J, Piñeiro MM. Thermal conductivity and viscosity measurements of ethylene glycol-based Al2O3 nanofluids. Nanoscale Res Lett 2011;6:221. doi:10.1186/1556-276X-6-221.

[52] Zhou JK. Differential transformation and its applications for electrical circuits 1986.

[53] Hatami M, Ganji DD. Motion of a spherical particle in a fluid forced vortex by DQM and DTM. Particuology 2014;16:206–12. doi:10.1016/j.partic.2014.01.001.

[54] Pourmehran O, Rahimi-Gorji M, Hatami M, Sahebi SAR, Domairry G. Numerical optimization of microchannel heat sink (MCHS) performance cooled by KKL based nanofluids in saturated porous medium. J Taiwan Inst Chem Eng 2015;55:49–68. doi:10.1016/j.jtice.2015.04.016.

[55] Hatami M, Ganji DD. Motion of a spherical particle on a rotating parabola using Lagrangian and high accuracy Multi-step Differential Transformation Method. Powder Technol 2014;258:94–8. doi:10.1016/j.powtec.2014.03.007.

[56] Dogonchi AS, Hatami M, Domairry G. Motion analysis of a spherical solid particle in plane Couette Newtonian fluid flow. Powder Technol 2015;274:186–92. doi:10.1016/j.powtec.2015.01.018.

[57] Hatami M, Sheikholeslami M, Domairry G. High accuracy analysis for motion of a spherical particle in plane Couette fluid flow by Multi-step Differential Transformation Method. Powder Technol 2014;260:59–67. doi:10.1016/j.powtec.2014.02.057.